Int. J. Solids Structures Vol. 19, No. 7, pp. 625–641, 1983
Printed in Great Britain.

0020-7683/83 $3.00 + .00
Pergamon Press Ltd.

DOUBLY SYMMETRIC INTERACTIVE BUCKLING OF PLATE STRUCTURES

SRINIVASAN SRIDHARAN
Associate Professor, Department of Civil Engineering, Washington University in St. Louis, MO 63130, U.S.A.

(*Received* 24 *March* 1982; *received for publication* 8 *November* 1982)

Abstract—A semianalytical approach is developed for the study of doubly symmetric interactive buckling of plate structures subject to axial compression, using the theory of mode interaction and finite strip concept. The approach is shown to be capable of dealing with a variety of interaction phenomena. Imperfection-sensitivity of a panel with near-coincident local and Euler critical stresses is seen to be dependent on the slenderness of the constituent members and the extent of their participation in the local buckling process. No catastrophic behavior is associated, however, with interactive buckling of a narrow stiffened plate supported along its longitudinal edges, in the elastic range. The "naive optimum" design is probably justified in these cases.

NOTATION

C extensional rigidity ($= Et/(1-\nu^2)$) of the plate element
D flexural rigidity ($= Et^3/12(1-\nu^2)$) of the plate element
E Young's Modulus
H operator relating the generic strain to generic stress
N_x, N_y, N_{xy} membrane stress resultants (Normal and shearing) acting at the middle surface of the plate
R ratio between overall and local critical stresses
U total potential energy
t thickness of plate element
l length of the plate structure
m_1, m_2 number of halfwaves of the buckling modes designated 1 and 2 respectively (Subscript 1 corresponds to a local mode always)
u, v, w the displacement components defined over the middle surface of the plate
x, y, z the coordinate directions (longitudinal, transverse and normal)
ϵ the generic strain
$\epsilon_x, \epsilon_y, \epsilon_{xy}$ normal and shearing strains at the middle surface of the plate element
λ_0 prescribed average axial strain (end shortening divided by length) of the structure
λ_1, λ_2 critical values of λ_0 (Subscript 1 corresponds to local mode)
λ_{max} the value of λ_0 at which the structure carries the maximum load
ν Poisson's ratio
ξ_1, ξ_2 amplitudes of the initial buckling in mode 1 and 2 respectively (normalized with respect to the plate thickness)
$\xi_1^{(0)}, \xi_2^{(0)}$ initial imperfections in the modes 1 and 2 respectively
σ_0 prebuckling stress
σ_e euler critical stress
σ_l local critical stress
σ_{c1}, σ_{c2} critical stresses in modes 1 and 2
σ_{av} average stress carried by the plate structure
σ_{max} maximum of σ_{av}

INTRODUCTION

Recent years have seen a surge of interest in the subject of interactive buckling of plate structures. This has largely been due to the discovery[1] of the fact of imperfection-sensitivity associated with "naive" optimum designs based on the equality of local and overall buckling strengths under axial compression. The interest has been focussed on the determination of the imperfection-sensitivity of near-coincident buckling and the ultimate strength of the structure for given ratios (R) of Euler buckling stress (σ_e) to the local buckling stress (σ_l).

Interaction of buckling modes in plate structures is not confined, however, to the problem of local and overall buckling. Prismatic plate structures with a variety of cross-sectional configurations are currently being employed in various forms of engineering construction. When subjected to axial compression these can buckle in a variety of modes which may be classified as below:

Mode I

Each constituent plate can buckle out of plane with the junctions remaining essentially straight. This is the familiar "local" buckling mode and has a halfwave length of the same order of magnitude as the width of the constituent plates (Fig. 1a).

Mode II

Some of the constituent plates may undergo inplane bending (and twisting) while the rest bend out of plane as in pure local buckling. This type of buckling has been termed "local torsional buckling", "stiffener buckling" or "orthotropic buckling" depending upon the context (Fig. 1b–c). The associated wavelengths are considerably greater than those of Mode I, but there is a halfwave length for which the critical stress is a minimum.

Mode III

The plate structure may buckle in an "overall" mode which may be either a purely flexural mode or a flexural torsional mode. This mode involves practically no bending in the cross-sectional plane.

Significant postbuckling resistance is generally available after local buckling where as the intervention of overall (Mode III) buckling generally paves the way for the exhaustion of the stiffness of the structure. Again the inplane bending of the stiffening elements which occurs in Mode II buckling often would lead to plastic yielding at key locations of the structure thus hastening the collapse of the structure. Any intervention of the latter two modes can therefore be expected to seriously undermine the often significant post-local-buckling strengths of plate structures.

In view of the foregoing remarks, the following interactions would appear to be of interest from an engineering stand point:

(1) A local mode (Mode I) with another local mode.
(2) Mode I with Mode II.
(3) Mode I with Mode III.

The problem of interaction of two local modes in a rectangular plate has been studied by Supple[2]. The interaction falls in the "doubly symmetric" category with a potential energy function for the perfect structure in the form:

$$U = \left(1 - \frac{\sigma}{\sigma_{c_1}}\right)\xi_1^2 + \left(1 - \frac{\sigma}{\sigma_{c_2}}\right)\xi_2^2 + b_{11}\xi_1^4 + b_{12}\xi_1^2\xi_2^2 + b_{22}\xi_2^4 \tag{1}$$

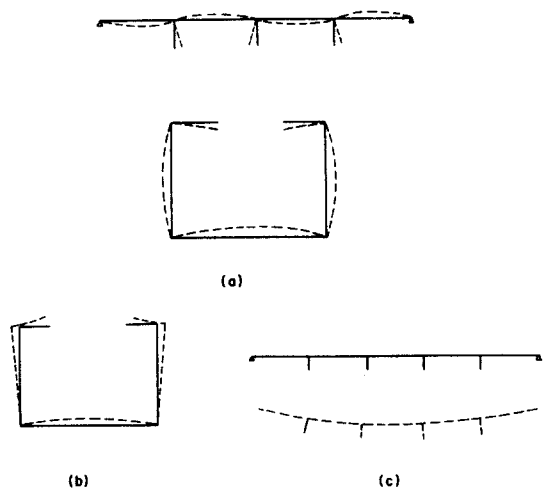

Fig. 1. Typical buckling modes of prismatic plate structures. (a) Local modes. (b) Local-torsional mode. (c) Orthotropic mode.

where 'σ' is the loading parameter (e.g. average stress carried by a uniformly compressed plate in Ref. [2]) ξ_1 and ξ_2 are the amplitudes of the participating modes of buckling, and σ_{c_1} and σ_{c_2} are the respective critical stresses. A detailed study of the general characteristics of such a system has been made by Supple in an earlier paper[3]. The energy function (1) is known to lead to the double cusp catastrophe[4] studied in some detail by Magnus and Poston[5, 6]. Such an energy function arises in stiffened structures whenever the buckling modes consists of even number of halfwaves, e.g. in stiffened cylindrical shells[7].

The first detailed investigations of nonlinear interaction between the overall buckling of built up column and local buckling of plate flanges are due to Graves-Smith[8] and van der Neut[9]. Several authors[10–15], notably Koiter, Tvergaard and Thompson among them contributed to further developments both for built up columns and stiffened plates. Tvergaard's paper[10] has received considerable attention on two counts: it is one of the earlier systematic attempts to employ the theory of mode interaction to study the problem, and his analysis predicted severe imperfection sensitivity for a panel having stocky stiffeners. However, in his calculations, Tvergaard neglected several terms which appear to have considerable importance in retrospect. His analysis is based on the semi-symmetric[16] energy function for the perfect structure in the form:

$$U = \left(1 - \frac{\sigma}{\sigma_{c_1}}\right)\xi_1^2 + \left(1 - \frac{\sigma}{\sigma_{c_2}}\right)\xi_2^2 + b_{112}\xi_1^2\xi_2 + b_{222}\xi_2^3 \tag{2}$$

where ξ_1 and ξ_2 stand here for the local and overall buckling amplitudes. Here the most important omission appears to be the quartic term in ξ_1, which encapsulates the post-local-buckling resistance. Again the retention of only the lowest order terms associated with imperfections in his analysis restricts the validity of his analysis to extremely small imperfections. Interestingly for the case of cross-sections with two axes of symmetry, Tvergaard model would predict neither an interaction nor the existence of postbuckling equilibrium in individual modes, as then both b_{112} and b_{222} will identically vanish.

Koiter developed a comprehensive, but a somewhat simplified method of approach to the interactive buckling in stiffened panels[11–13]. In plate structures, the interaction of long-wave mode (such as the Euler mode) with a local mode triggers two additional neighboring modes (as shown in the present paper in a later section) and these in turn trigger additional modes thus setting up a chain reaction. In stiffened plates this phenomenon takes the form of "amplitude modulation" and Koiter accounted for this by letting the local amplitude vary according to a slowly varying function. His energy functional takes the form:

$$U = \left(1 - \frac{\sigma}{\sigma_{c_1}}\right)\xi_1^2 + \left(1 - \frac{\sigma}{\sigma_{c_2}}\right)\xi_2^2 + b_{112}\xi_1^2\xi_2 + b_{1111}\xi_1^4 \tag{3}$$

where 'ξ_1' is no longer simply the amplitude of the local mode, but includes the effect of the modulating function. In calculations Koiter included some of the higher order terms of initial imperfections. The interaction of the buckling modes occurs by virtue of the term involving $\xi_1^2\xi_2$. It is important to note that this does not vanish for the multibay column which buckles in even number of halfwaves, because of amplitude modulation, but it does however, vanish when the cross-section has two axes of symmetry and the local mode is symmetric or antisymmetric about the axis about which overall buckling takes place because of the antisymmetry of the overall displacements in the cross-section about the same axis (Fig. 2). In order to explain the interaction in such cases Koiter has suggested the consideration of the modification of the local mode that occurs in the postbuckling range.

In the present paper a method of approach is outlined wherein this modification in the postbuckled range is automatically comprehended in a systematic application of the theory of mode interaction[7]. In order to highlight this feature, we consider the situation where the cubic terms vanish because of symmetry. Thus we are constrained to consider the

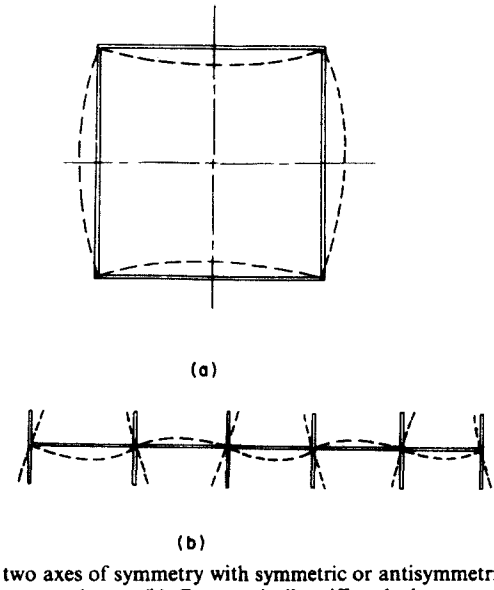

Fig. 2. Sections with two axes of symmetry with symmetric or antisymmetric local modes. (a) Box column. (b) Concentrically stiffened plate.

quartic terms in the analysis and our model reduces to the doubly symmetric one mentioned earlier. In axially compressed prismatic plate assemblies, this model is applicable in the following situations:

(i) Both the participating modes consist of even number of halfwaves. Note that a column clamped at the ends can be visualized as one with halfwaves of overall buckling (Fig. 3a).

(ii) The cross-section of the column has two axes of symmetry and carries a uniform compressive stress. The overall buckling may consist of a single halfwave (corresponding to the simply supported end conditions), while the local buckling must however consist of an even number of halfwaves. (The latter restriction can in practical computations be relaxed since the local buckling can be modelled using the "classical assumptions" [17] first suggested by Benthem [18]).

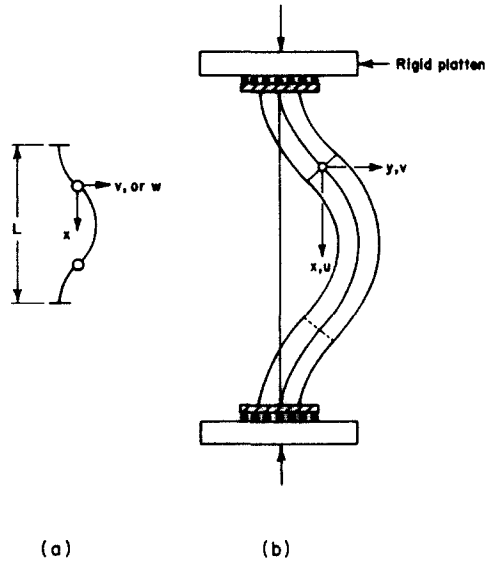

Fig. 3. Idealization of the end boundary conditions. (a) Initial buckling mode of a column clamped at its ends. (b) Inplane buckling of a stiffener and a possible loading arrangement.

The doubly symmetric interaction considered in the paper involves principally two modes and the amplitude modulation arises by virtue of the mixed second order field taken into account in the analysis. The paper demonstrates the value of the semianalytical technique which employs the characteristic functions of the postbuckling problem to describe the variation of displacements in the longitudinal direction and discretization in the transverse direction to be able to model complex cross-sectional geometries. The use of the theory of mode-interaction provides a clear insight into the mechanics of the phenomena—a feature absent in the full-blown nonlinear analysis. The major limitation of the analysis stems from the fact that it is based on no higher than second-order displacement fields. If the load parameter approaches the singularities of the second order fields (in particular the mixed second order field for local and Euler buckling interaction) a severe imperfection sensitivity would be predicted. This would happen for instance, in the case of a near-perfect stiffened panel with near-coincident local critical loads associated with similar mode-shapes in the transverse direction. The Tvergaard panel is a case in point. An upper-bound to the maximum load carried can, however, be obtained by deactivising the secondary local modes by deleting the key term associated with the load parameter which is the source of the singularities.

The present studies clearly demonstrate the effect of slenderness of the stiffening elements on the imperfection-sensitivity of Euler-local buckling interaction: The more slender the stiffener, the more severe the imperfection-sensitivity. The interaction of local buckling and Mode II type of buckling for a narrow longitudinally supported panel carrying a single stiffener is also investigated. If the material remains elastic, this type of interaction does not produce any catastrophic behavior in presence of initial imperfections, i.e. there exists no limit to the end-compression the structure can carry. The "naive" optimum design concept appears to be justified here. On the otherhand, the appearance of overall deflections would result in a rapid build up of compressive stresses in key locations leading to an early onset of plasticity in practical cases. Interestingly, this tendency can be marginally offset by the presence of local imperfections.

THEORY

Figure 4 shows a typical plate structure divided into an appropriate number of strips together with the coordinate axes for a typical strip; the structure is assumed to be compressed uniformly.

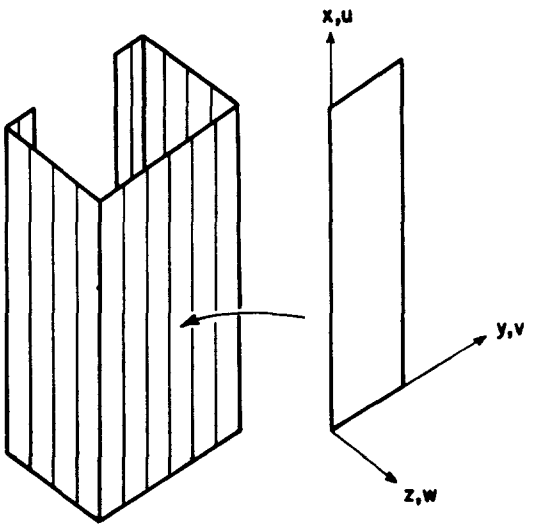

Fig. 4. Finite strip configuration and the local coordinate system and a typical strip.

Theoretical basis

In outlining the theory of mode interaction as developed for the present problem, we follow in the main, the elegant formalism employed by Budiansky and Hutchinson[19], and more recently by Byskov and Hutchinson[7].

Let $\bar{u}$ stand for a vector function defined by the displacement components u, v, w of the middle surface of a typical strip of a plate (Fig. 4) and be represented in the form:

$$\bar{u} = u_0 + u_1\xi_1 + u_2\xi_2 + u_{11}\xi_1^2 + u_{22}\xi_2^2 + u_{12}\xi_1\xi_2. \tag{4}$$

Here u_0 stands for the uniform uniaxial compression corresponding to the trivial primary path given by

$$u_0 = \begin{Bmatrix} \lambda_0(l/2 - x) \\ \nu\lambda_0 y \\ 0 \end{Bmatrix} \tag{5}$$

where λ_0 stands for the compressive strain imposed on the structure.

ξ_i are the nondimensional amplitudes of the participating buckling modes.

u_{11}, u_{22} are the respective second order displacement fields and $u_{21}(=u_{12})$ is the mixed second order field defined over the plate middle surface. The modes u_1 and u_2 are orthogonal in the sense the quadratic part of the potential energy takes a diagonalized form. The displacement fields are orthogonal to u_i in the sense

$$\int_A \lambda_0 \frac{\partial u_i}{\partial x}\frac{\partial u_{jk}}{\partial x}\,\mathrm{d}A = 0 \tag{6}$$

for any i, j, k, where the integral is taken over the area of the middle of the plate structure.

Let 'ϵ' stand for the generic strain characterized by the membrane strains (ϵ_x, ϵ_y, ϵ_{xy}) and curvatures (χ_x, χ_y, χ_{xy}), i.e.

$$\epsilon = \begin{Bmatrix} \epsilon_x \\ \epsilon_y \\ \gamma_{xy} \\ \chi_x \\ \chi_y \\ \chi_{xy} \end{Bmatrix}. \tag{7}$$

The description of 'ϵ' in the primary path takes the form:

$$\epsilon_0 = \{-\lambda_0\ \nu\lambda_0\ 0\ 0\ 0\ 0\}^T.$$

The first and higher order strain fields describing the bifurcated path take the form:

$$\epsilon_i = L_1(u_i) \tag{8a}$$

$$\epsilon_{ii} = L_1(u_{ii}) + \tfrac{1}{2}L_2(u_i) \tag{8b}$$

$$\epsilon_{ij} = L_1(u_{ij}) + L_{11}(u_i, u_j), \quad (i \neq j), \tag{8c}$$

etc. where L_1, L_2 L_{11} stand for appropriate linear, quadratic and bilinear operators.

The corresponding stress fields are obtainable from the linearized Hooke's law, stated simply as

$$\sigma = H\epsilon \tag{9}$$

The potential energy function for the eigenvalue and higher order field problems take the forms:

$$U_i = \tfrac{1}{2}\{H[L_1(u_i) \cdot L_1(u_i)] + \sigma_0^* \cdot L_2(u_i)\} \tag{10a}$$

(no sum on 'i')

$$U_{ii} = \tfrac{1}{2}\{H[L_1(u_{ii}) \cdot L_1(u_{ii}) + L_1(u_{ii}) \cdot L_2(u_i) + L_1(u_i) \cdot L_{11}(u_i, u_{ii})] + \sigma_0^* \cdot L_2(u_{ii})\} \tag{10b}$$

(no sum on 'i')

$$\underset{(i \neq j)}{U_{ij}} = \tfrac{1}{2}\{H[L_1(u_{ij}) \cdot L_1(u_{ij}) + L_1(u_{ij}) \cdot L_{11}(u_i, u_j) + L_1(u_i) \cdot L_{11}(u_j, u_{ij}) + L_1(u_j) \cdot L_{11}(u_i, u_{ij})] + \sigma_0^* \cdot L_2(u_{ij})\} \tag{10c}$$

(no sum on i or j)

where $\sigma_0^* = -\sigma_0 = -H\epsilon_0$. In the foregoing a dot operation indicates a product of two functions integrated over the area of the middle surface of plate structure. The principle of stationary potential is invoked to produce the necessary equilibrium equations to obtain u_i and u_{ij}.

The total potential energy function for prescribed axial compression can be written in the form:

$$U_{\text{Total}} = \tfrac{1}{2}\sigma \cdot \epsilon = \tfrac{1}{2}H\epsilon \cdot \epsilon \tag{11}$$

where

$$\epsilon = \epsilon_0 + \epsilon_1\xi_1 + \epsilon_2\xi_2 + \epsilon_{11}\xi_1^2 + \epsilon_{22}\xi_2^2 + \epsilon_{12}\xi_1\xi_2 + \epsilon_{112}\xi_1^2 + \epsilon_{221}\xi_2^2\xi_1.$$

In terms of the amplitudes ξ_1 and ξ_2,

$$U_{\text{Total}} = \tfrac{1}{2}\{[H\epsilon_1 \cdot \epsilon_1 - \sigma_0 \cdot \epsilon_{11}]\xi_1^2 + [H\epsilon_2 \cdot \epsilon_2 - \sigma_0\epsilon_{22}]\xi_2^2 + H[\epsilon_{11} \cdot \epsilon_{11}\xi_1^4 + \epsilon_{22} \cdot \epsilon_{22}\xi_2^4 + (2\epsilon_{11} \cdot \epsilon_{22} + \epsilon_{12} \cdot \epsilon_{12} + 2\epsilon_{112} \cdot \epsilon_2 + 2\epsilon_{221} \cdot \epsilon_1)\xi_1^2\xi_2^2]\}. \tag{12}$$

The influence of initial imperfections in the modes of buckling, $\xi_1^{(0)}$ and $\xi_2^{(0)}$, is incorporated by writing the strain field 'ϵ' in the form:

$$\epsilon = \epsilon_0 + \epsilon_1\xi_1 + \epsilon_2\xi_2 + \epsilon_{11}\{\xi_1^2 + 2\xi_1^{(0)}\xi_1\} + \epsilon_{22}\{\xi_2^2 + 2\xi_2^{(0)}\xi_2\} + \epsilon_{12}\{\xi_1\xi_2 + \xi_1^{(0)}\xi_2 + \xi_2^{(0)}\xi_1\} + \epsilon_{112}\{\xi_1^2\xi_2 + 2\xi_1\xi_1^{(0)}\xi_2 + \xi_1^2\xi_2^{(0)}\} + \epsilon_{221}\{\xi_1^2\xi_2 + 2\xi_2\xi_2^{(0)}\xi_1 + \xi_2^2\xi_1^{(0)}\}. \tag{13}$$

This is substituted in eqn (11) to produce a modified potential energy function in the form:

$$U_{\text{Total}} = (\lambda_1 - \lambda_0)a_1\xi_1^2 + (\lambda_2 - \lambda_0)a_2\xi_2^2 + b_{11}(\xi_1^4 + 4\xi_1^3\xi_1^{(0)} + 4\xi_1^2\xi_1^{(0)2}) + b_{22}(\xi_2^4 + 4\xi_2^3\xi_2^{(0)} + 4\xi_2^2\xi_2^{(0)2}) + b_{12}\xi_1^2\xi_2^2 + c_{12}\xi_1^2\xi_2\xi_2^{(0)} + c'_{12}\xi_2^2\xi_1\xi_1^{(0)} + d_{12}(\xi_1^2\xi_2^{(0)2} + \xi_2^2\xi_1^{(0)2}) + e_{12}\xi_1\xi_2\xi_1^{(0)}\xi_2^{(0)} - 2\lambda_0(a_1\xi_1\xi_1^{(0)} + a_2\xi_2\xi_2^{(0)}) \tag{14}$$

where $a_1, a_2 \ldots e_{12}$ are coefficients evaluated using eqn (9) and (13), λ is the prescribed end shortening divided by the length of the structure, λ_1 and λ_2 are the critical values of λ_0 in the modes 1 and 2. By differentiating eqn (11) with respect to each of ξ_1 and ξ_2, a pair of nonlinear equations are produced which is solved iteratively for values of λ_0 incremented in small steps.

Solution of the component problems

The halfwave length of local buckling is generally so small compared to the length of the structure so that some approximation of the end boundary conditions can often be

accepted. Because of this, it is possible to represent the displacements in the longitudinal direction by their characteristic forms which satisfy the governing differential equations. A semianalytical technique is therefore employed with discretization confined to the transverse direction.

x-variation of the displacement fields

Figure 4 shows a typical plate structure divided into a number of longitudinal strips. The functions describing the variation of the displacements u, v and w in the longitudinal direction are derived from the differential equations governing the problem which in turn can be obtained as Euler equations associated with the potential energy functional. For the case of prescribed end compression, the total potential energy reduces to the total internal strain energy. The middle surface strains and displacements are taken in the form:

$$\epsilon_x = u_{,x} + \tfrac{1}{2}\{(w_{,x})^2 + \underline{(v_{,x})^2}\} \tag{15a}$$

$$\epsilon_y = v_{,y} + \tfrac{1}{2}\{(w_{,y})^2 + (v_{,y})^2\} \tag{15b}$$

$$\gamma_{xy} = u_{,y} + v_{,x} + w_{,x}w_{,y} + v_{,x}v_{,y}. \tag{15c}$$

The above relations differ from those employed in classical plate theory by the presence of the nonlinear term in v, the inplane displacement in the transverse direction. Of the nonlinear terms in 'v', the most significant is the underlined term $\frac{1}{2}(v_{,x})^2$ in eqn 15(a) which plays a crucial role in modelling buckling involving significant inplane movements of constituent plates[20]. The other nonlinear terms involving $v_{,y}$ (eqn 15b, c) can be safely discarded as the inplane bending of the plate elements resembles closely the rigid body translations of cross section. Thus modified, the strain-displacement relations are used in expressing the strain energy functional in terms of displacements. The corresponding Euler equations for a typical plate take the form:

$$N_{x,x} + N_{xy,y} = 0 \tag{16a}$$

$$N_{xy,x} + N_{y,y} + N_x v_{,xx} + N_{x,x}v_{,x} = 0 \tag{16b}$$

$$D\nabla^4 w - (N_x w_{,xx} + 2N_{xy}w_{,xy} + N_y w_{,yy}) = 0. \tag{16c}$$

In the foregoing N_x, N_y and N_{xy} are stress resultants related to the strains as follows:

$$N_x = C\{\epsilon_x + \nu\epsilon_y\} \tag{17a}$$

$$N_y = C\{\epsilon_y + \nu\epsilon_x\} \tag{17b}$$

$$N_{xy} = C\frac{(1-\nu)}{2}\nu_{xy} \tag{17c}$$

and $C = Et/(1-\nu^2)$ and $D = Et^3/12(1-\nu^2)$, t being the thickness.

In order to obtain an insight into the nature of solution of these differential equations we employ a perturbation technique and produce ordered sets of sequentially linear equations. We consider in particular the case of plate structures which carry prescribed compression by rigid end plattens so that the axial stress may be taken in the form:

$$N_x = -Et\lambda_0 + \bar{N}_x \tag{18}$$

where $\bar{N}_x$ is the modification of the axial stress in the bifurcated state. Taking the stress resultants and displacements in the form of eqn (4), the eigen value problem for the critical stresses and buckling modes yields the following solutions for the displacements[17]:

$$u_i = \bar{u}_i(y)\cos\left(\frac{m_i\pi x}{l}\right) \tag{19a}$$

$$v_i = \bar{v}_i(y)\sin\left(\frac{m_i\pi x}{l}\right) \tag{19b}$$

$$w_i = \bar{w}_i(y)\sin\left(\frac{m_i\pi x}{l}\right) \tag{19c}$$

where 'i' takes the values 1 or 2 and thus identifies a participating buckling mode, m_i gives the number of halfwaves of the buckling mode and $\bar{u}_i(y)$, etc. are appropriate functions of 'y', the transverse coordinate of the plate.

The second order displacement field for each mode can be extracted from the governing equations with the aid of the perturbation technique[20] in the form:

$$u_{ii} = \bar{u}_{ii}(y)\sin\left(\frac{2m_i\pi x}{l}\right) \tag{20a}$$

$$v_{ii} = \bar{v}_{ii,0}(y) + \bar{v}_{ii,2}(y)\cos\left(\frac{2m_i\pi x}{l}\right) \tag{20b}$$

$$w_{ii} = \bar{w}_{ii,0}(y) + \bar{w}_{ii,2}(y)\cos\left(\frac{2m_i\pi x}{l}\right). \tag{20c}$$

Finally the mixed second order displacement field can similarly be obtained in the form

$$u_{12} = u^*_{12}(y)\sin\frac{(m_1 - m_2)\pi x}{l} + \bar{u}_{12}(y)\sin\frac{(m_1 + m_2)\pi x}{l} \tag{21a}$$

$$v_{12} = v^*_{12}(y)\cos\frac{(m_1 - m_2)\pi x}{l} + \bar{v}_{12}(y)\cos\frac{(m_1 + m_2)\pi x}{l} \tag{21b}$$

$$w_{12} = w^*_{12}(y)\cos\frac{(m_1 - m_2)\pi x}{l} + \bar{w}_{12}(y)\cos\frac{(m_1 + m_2)\pi x}{l}. \tag{21c}$$

In the foregoing the starred end barred quantities are again, appropriate functions of 'y' which are determined using a finite strip analysis.

Loading and end boundary conditions

Figure 3(b) shows the variation of displacements of a typical member undergoing inplane buckling. The structure may be thought of as being compressed by rigid plattens at the sections of the plane of symmetry. At these planes the section is free to distort but no rotations relative to the plattens is allowed to occur; also the shear stresses at these cross-sections vanish. Thus the analysis treats of a case in which the plattens are completely frictionless. When one of the participating modes takes the form of a purely local mode (Mode I), the corresponding halfwave length is generally so small compared to the length of the structure that any errors introduced by deviations from the assumed end conditions would be of little consequence as long as the structure is uniformly compressed. Again when a participating mode takes the form of Euler buckling, the contribution of the corresponding second order displacements v_{ii} and w_{ii} are sufficiently small in order for the analysis to be applicable to a column clamped at its ends.

Displacement functions in the transverse direction

The eqns (19)–(21) give the variation of the displacements in the longitudinal direction. Each of the functions of 'y' appearing in the description of inplane displacements are taken

to be linear whereas cubic functions associated with four degrees of freedom are employed in the description of normal displacements across the strips.

Some remarks on the solution procedure

With the aid of displacement functions it is possible to set up the stiffness matrices for the eigenvalue problems using the potential energy functions given by eqn (10a) and the well known finite strip technique. The corresponding eigen vectors are normalized with respect to the maxima of the magnitudes of displacements or the values at key locations. In the determination of second order displacement fields, it is first observed that the potential energy functions contain terms which are quadratic or bilinear in the first order quantities which produce the nonzero right hand side of the equilibrium equations. The eigen vectors and the associated x-variations are used as inputs in the building up of the said right hand side term. Note that in each of the second order field problems, the participating harmonics (0 and $2mi$ or $(m_1 + m_2)$ and $(m_1 - m_2)$) are uncoupled in the solution process thus greatly simplifying the computation.

The secondary local modes

The solution of the second order fields is governed by λ_0, the nondimensional end-shortening of the column and load parameter, even though it is often sufficient to set a constant value for it in the calculations. Since our object is the determination of the maximum load the structure can carry for a given level of imperfections, the chosen value for λ_0 must not exceed λ_{max} the value at which the maximum load is attained by the structure. For computations, trial analyses with progressively modified values of λ_0 are performed till $\lambda_0 = \lambda_{max}$ within an error of 1%. (Such an analysis which takes due account of geometric stiffness terms will be henceforth referred to as Analysis I.)

The displacement functions of the mixed second-order field have a harmonic variation in the x-direction and have the same number of half-waves as the primary local mode but for a difference of $\pm m_2$. As a result the field often has singularities at values of λ_0 close to λ_1—these corresponding to the buckling of the structure with the half-wave lengths of the displacement functions. Thus as $\lambda_0 \to \lambda_1$ there would result an exaggeration of the importance of the mixed second-order field because of the absence of the stabilizing influence of the still higher order terms neglected here. A high sensitivity to small imperfections is therefore predicted in such cases. An upperbound to the maximum load carried for a given level of imperfections is, however, easily obtained by neglecting the geometric stiffness terms contained in eqn (10c) viz. $\lambda_0 \cdot L_2(u_{12})$ which triggers these secondary local modes. (Such an analysis which neglects the geometric stiffness effects in the determination of the second order fields will be henceforth referred to as Analysis II.)

EXAMPLES

The significance of doubly symmetric interaction in practical plate structures is now illustrated by the following examples:

(i) The interaction of two modes of buckling in a simply supported rectangular plate having an aspect ratio of 2. Note this problem has been studied by Supple using an analytical approach and his results are used to illustrate the convergence and accuracy of the present solutions.

(ii) The interaction of local and overall buckling in wide eccentrically stiffened panels—a subject of current interest

and

(iii) The interaction of local and overall (more specifically Mode II type of buckling) in a narrow plate simply supported along its longitudinal edges and carrying a single eccentric stiffener. No theoretical study of such a problem appears to have been made so far.

(i) *Mode interaction in a rectangular plate*

Figure 5 shows a plate having an aspect ratio of 2. The plate is assumed to be simply supported with the longitudinal edges allowed to move but held straight. Interaction between two modes, one having two halfwaves and the other with three halfwaves in the longitudinal direction (i.e. $m_1 = 2$, $m_2 = 3$) is studied. As mentioned already, this problem has been studied by Supple who showed that apart from the two uncoupled equilibrium paths emanating from the respective critical stresses, there exists a coupled equilibrium path which takes the form a rising curve (whose projection is a hyperbola in the ξ_1-ξ_2 plane) branching from the secondary buckling path, i.e. the equilibrium path corresponding to the higher critical stress (Fig. 6). When the initial imperfections in the form of either mode are present, the buckling mode is a coupled one from the start of the loading, but the influence of one of the modes tends to predominate as loading progresses.

These conclusions are confirmed by the present study which apparently has taken a different route. Figure 7(a–c) shows a comparison of our results obtained with 8 elements and 24 elements in half the plate for four sets of initial imperfection in the two modes. Attention has been restricted to natural loading paths and complementary equilibrium paths are not indicated. The convergence of the results are seen to be remarkably good with the coarser discretization yielding results of sufficient accuracy.

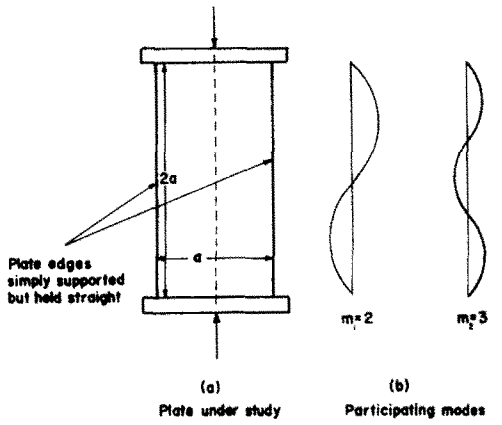

Fig. 5. The details of the plate investigated. (a) Plate under study. (b) Participating modes.

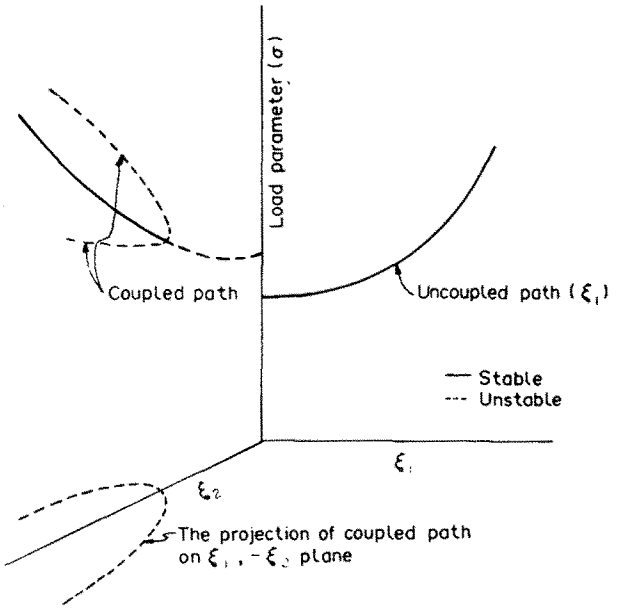

Fig. 6. Equilibrium paths of the perfect plate under interaction of two local modes.

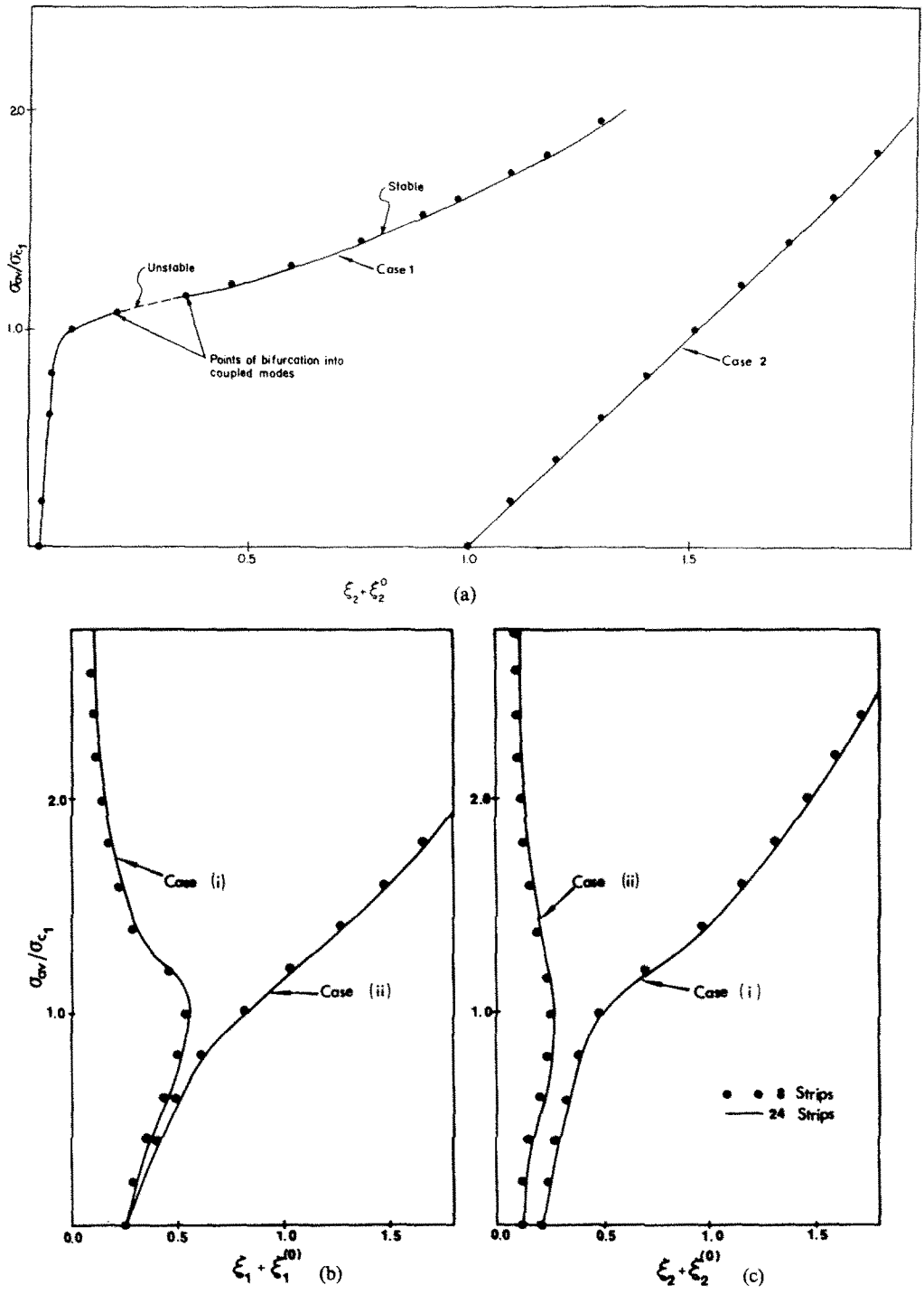

Fig. 7.(a) Relationship between the deflection amplitudes (divided by t) and the average stress carried by the plate for imperfections in the second buckling mode (i) $\xi_2^{(0)} = 0.02$, $\xi_1^{(0)} = 0.0$; (ii) $\xi_2^{(0)} = 1.0$, $\xi_1^{(0)} = 0.0$. (b, c) Relationship between the deflection amplitudes (divided by t) and the average stress carried by the plate for case (i) $\xi_1^{(0)} = 0.25$, $\xi_2^{(0)} = 0.20$ and case (ii) $\xi_1^{(0)} = 0.25$, $\xi_2^{(0)} = 0.125$.

Interaction of local and overall buckling in wide stiffened panels

Figure 8 shows a wide integrally stiffened plate. Because of symmetry with respect to longitudinal centre lines of each panel, only the action of a typical panel included between two successive centre lines is considered. As discussed earlier, the present analysis closely models the clamped end conditions.

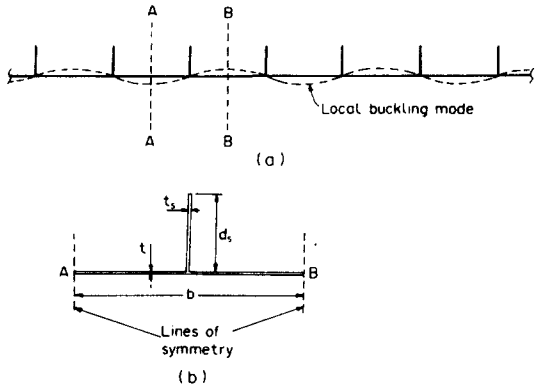

Fig. 8. Wide integrally stiffened plate. (a) Local buckling mode. (b) Dimension of a typical panel.

Three types of panels are considered in the present study. Table 1 summarizes the details of the same. Of these Panel A has a comparatively slender stiffener ($d_s/t = 25$) and thus initiates the buckling process; Panel A' has the same cross-section as Panel A but has a reduced length so that $\lambda_1/\lambda_2 \simeq 1.5$. Panel B has a stiffer web ($d_s/t = 15$) typically used in offshore construction. Panel C has a stocky stiffener of the type preferred in aerospace industry, previously investigated by Tvergaard. In all the cases the overall mode is assumed to consist of two half-waves to correspond with the boundary conditions indicated in Fig. 3 while the local mode consists of an even number of half-waves.

A common feature of the behavior of Panels A, B and C is the existence of a limit on the end-shortening on the natural loading path in presence of imperfections. For the perfect structure the coupled equilibrium path takes the form of a descending hyperbola branching off the primary buckling path (that corresponding to the lower critical load) rendering it unstable. Thus in general a catastrophic failure occurs by snap through to remote equilibrium path. Exceptions to this trend are found in the response predicted for higher levels of imperfections (and in particular by the upper bound solution) where failure occurs by the attainment of the maximum load, but not of end-shortening. Thus in these cases, no loss of stability occurs as the structure begins to shed the load—a gradual process of failure indeed.

Figure 9(a–c) shows the imperfection-sensitivity surfaces of panels A, A′ and B as given by the Analysis I. The cases of A and B are those of near-coincident buckling. The surfaces give the maximum load carried by the structure as a fraction of the lower of the critical loads of the participating modes. The figures in addition show outlines of the imperfection-sensitivity surfaces as given by Analysis II. Panel A is seen to be considerably more imperfection-sensitive than Panel B, the reduction of the load carrying capacity for a local imperfection of 0.25t (t being the thickness of the plate) in the case of Panel A being more

Table 1*.

Identification of Panel	Geometry					Buckling modes** and critical stresses			
	b	t	d_s	t_s	ℓ	m_1 (local)	m_2 (overall)	$\sigma_{c_1}/E \times 10^3$	$\sigma_{c_2}/E \times 10^3$
A	50	1	25	1	1320	22	2	1.157	1.190
B	50	1	15	1	600	12	2	1.526	1.513
C	113.6	1	11.36	4.544	908.8	12	2	0.475	0.473
A'	50	1	25	1	1080	18	2	1.157	1.762
C'	113.6	1	11.36	4.544	757.3	10	2	0.475	0.645

*The notation is explained in Fig. 8

**Subscripts 1 and 2 refer to local and overall modes.

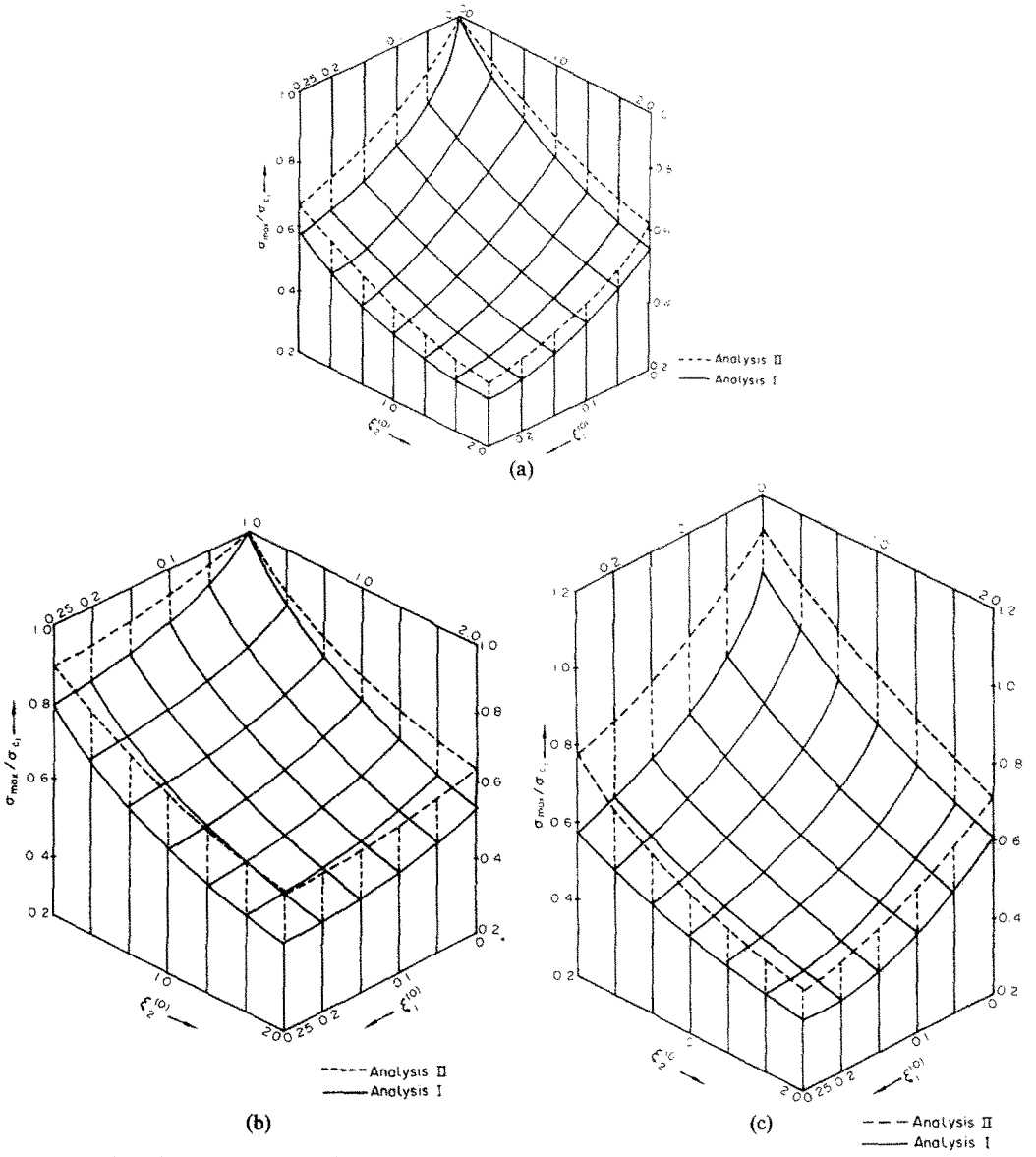

Fig. 9.(a) Imperfection-sensitivity surface of panels A (vide Table 1) (imperfection-amplitudes are rendered dimensionless by division by plate thickness). (b) Imperfection-sensitivity surface of panel B (vide Table 1). (c) Imperfection-sensitivity surface of panel A' (vide Table 1).

than twice that for Panel B. Again the sensitivity to overall imperfections (measured in terms of the ratio of the corresponding imperfection amplitude to the length of the structure) is much less severe in the case of Panel B.

The explanation of the severe imperfection-sensitivity of Panel A lies in the significant modification in the initial buckling suffered by the cross-section and in particular by the stiffener signified by the displacement w_{12} which arises as a result of overall compression working over the local deformation. This effect is contained in the term $\partial u_2/\partial x \cdot \partial w_1/\partial_x \cdot \partial w_{12}/\partial x$ (corresponding to $L_1(u_2) \cdot L_{11}(u_1, u_{12})$ of eqn. 10c) of the energy function—a term ignored in the previous investigations. The same reasoning applies for Panel A' (Fig. 9b)—a case of well-separated critical loads—for which imperfection-sensitivity is still severe.

The presence of local imperfections on the whole, accentuates the difference between the two solutions based on Analysis I and II respectively. This is due to the triggering of the secondary local modes at an early stage in the loading process. Again Analysis I predicts a high degree of sensitivity to minute imperfections. As imperfections become

smaller and smaller, λ_{max} approaches λ_1 and the secondary local modes contained in the mixed second order field become highly activated. Especially so in this case, as it is seen that the mixed second order field is, in the transverse direction, antisymmetric with reference to the stiffeners—a form which closely resembles the eigen modes of the singularities of the field itself. This feature of the stiffened panel problem has the greatest significance in the prediction of the behavior of Panel A′. Even though the critical loads are well separated in this case ($R \simeq 1.5$) the maximum load predicted for the perfect structure by Analysis I is no higher than the local critical load itself. This is in contrast to an increase of about 10% over the local critical load predicted by Analysis II.

The Tvergaard panel (ref. Fig. 10) illustrates how much the two solutions can differ in their assessment of sensitivity to local imperfections. Significantly the results of Analysis II (the upper bound analysis) are in closer agreement with Koiter's solution for the multibay panel[12]. Again Analysis II indicates that an increase of λ_1/λ_2 to 1.33 by a suitable reduction in length (vide Panel C′, Table 1) almost wipes out the sensitivity to local imperfections and the maximum average stress remains unaltered (at $1.26\,\lambda_1 E$) whatever the magnitude of local imperfections (not illustrated). This trend is in qualitative agreement with Koiter's prediction for the multi-bay column. The overall imperfections, however, continue to have a dominating influence on the behavior of the column.

Example of a narrow plate with an intermediate stiffener

A stiffened plate carrying a single central stiffener is indicated in Fig. 11. The plate is simply supported all along its edges but the longitudinal edges are free to wave in the plane of the plate. These boundary conditions closely model the top flange of a box beam. The interaction of the purely local mode (Mode I) and the overall mode which involves inplane

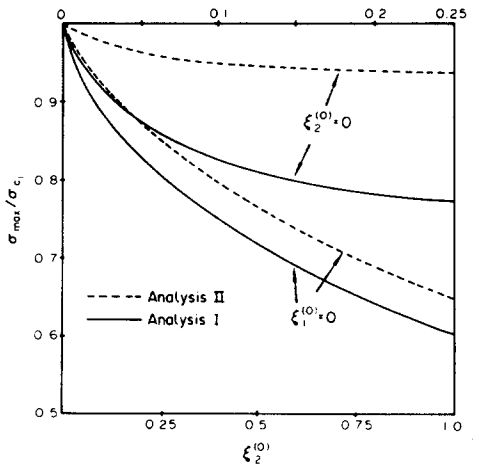

Fig. 10. Imperfection-sensitivity of Tvergaard panel (Panel C).

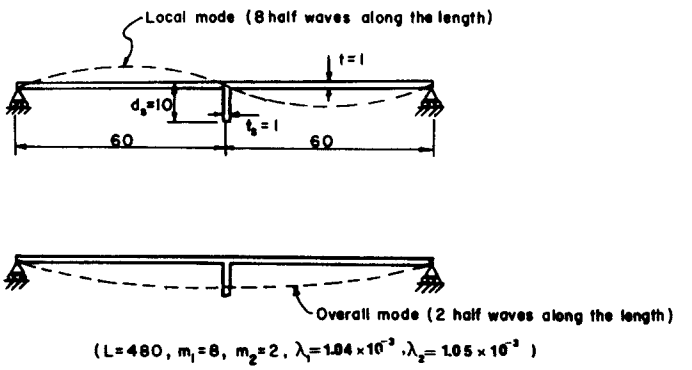

Fig. 11. Details of the narrow stiffened plate studied.

movement of the stiffener (Mode II) is investigated for certain combinations of initial imperfections. The case considered is one of near coincident buckling with the critical stress of Mode II exceeding that of Mode I by 1% ($R \simeq 1.01$).

The interaction of the two modes of buckling considered does not produce any catastrophic effects unlike the local-Euler buckling interaction. Analysis I (based on setting $\lambda_0 = \lambda_1$) indicates that the coupled mode for the perfect structure takes the form of an ascending hyperbola branching from the equilibrium path associated with the lower critical load. Thus in this case, the local buckling which occurs first, is soon followed by bifurcation into the coupled mode. Figure 12(a, b) shows the plots of amplitudes of the two modes against the average stress carried by the structure for different combinations of imperfections. It is seen that when imperfection in only one mode is present, there occurs always a bifurcation to the coupled mode. With combined imperfections, there is no instability at all. Both the analyses give the same result when imperfections in only one of the modes is present, though they differ slightly in the prediction of stability of equilibrium. Some differences, however, are noticed in the responses predicted by the two analyses for combined imperfections (Fig. 12a, b). The final picture is the same whatever the type of analysis or the nature of imperfections: there exists a stable rising equilibrium path and this does involve the overall buckling (Mode II) displacements.

The appearance of overall buckling displacements does not exhaust the stiffness or lead to a levelling off of the load carried by the structure as long as the structure remains elastic. In a practical metal structure, there would occur plastic yielding at the stiffener tip because of the rapid build up of compressive stresses which follows the inplane movement of the stiffener. The presence of local imperfections tends to reduce the overall deflections—unlike the case of local-Euler buckling interaction—thus leading to a higher first yield load for a given level of imperfection in Mode II. With the onset of plasticity a rapid deterioration of the stiffness of the structure can be expected. Thus there still appears to be an advantage in designing for a higher value of R.

CONCLUSIONS

A doubly symmetric model is proposed for the interactive buckling of prismatic plate structures subjected to uniform end compression. Typical cases of interaction that can arise

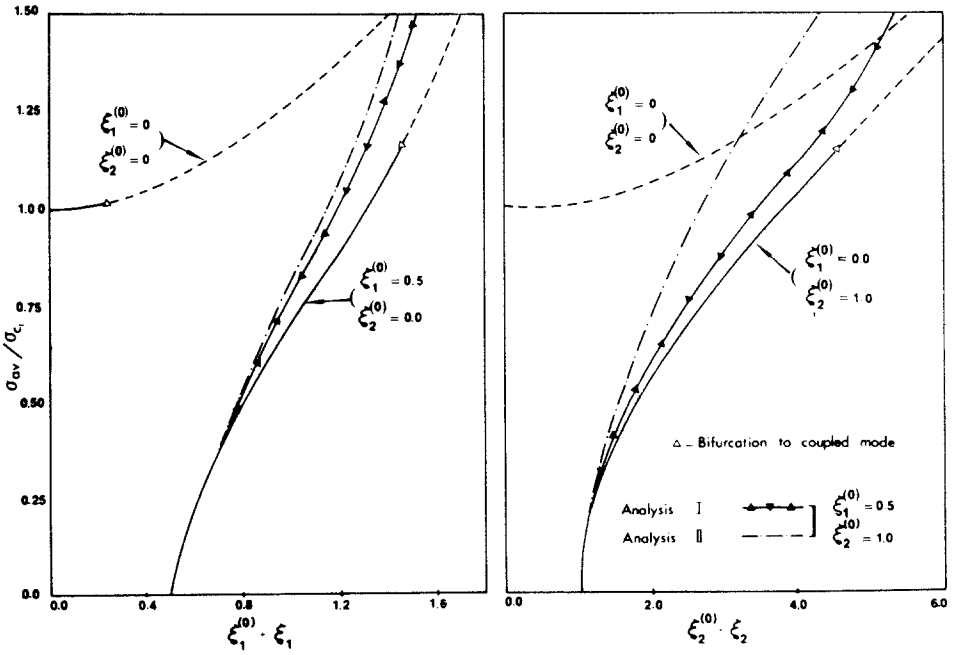

Fig. 12.(a) Load vs Local buckling amplitude ($\xi_1 + \xi_1^{(0)}$) for the plate in Fig. 11. (b) Load vs Mode II buckling amplitude ($\xi_2 + \xi_2^{(0)}$) for the plate in Fig. 11.

in prismatic plate structures are considered. The use of a semianalytical technique makes it possible to consider a variety of cross-sectional geometries with considerable ease.

Under coincident buckling the wide stiffened plates studied here exhibit imperfection-sensitivity in proportion to the slenderness of the stiffeners. The imperfection-sensitivity is significantly influenced by a key term in the energy function not considered in the previous investigations. The paper draws attention to the analytical difficulties associated with the presence of singularities of the mixed second order field close to the primary critical local end compression. An upperbound estimate of the stiffness of the structure is therefore obtained by the neglect of the geometric stiffness terms of the second order fields. The results of such an analysis for the Tvergaard panel are in closer agreement with those of Koiter[12].

In the case of narrow stiffened plates supported along the longitudinal edges, no catastrophic failure is seen to occur in presence of initial imperfections, provided elastic behavior is assured. In practical cases, the presence of overall imperfections would lead to early onset of plasticity leading to serious loss of stiffness. Interestingly the presence of local imperfections can be of beneficial influence here in that they tend to reduce the overall deflections, thus delaying the onset of plasticity.

Acknowledgements—The paper is an outcome of an ongoing research program supported in part by grant from NSF (grant CEE–8204673) and in part by the Department of Civil Engineering, Washington University in St. Louis. The author wishes to thank Prof. Phillip L. Gould, Chairman of the department for his encouragement and interest in the work.

REFERENCES

1. W. T. Koiter and M. Skaloud, Interventions. *Comportment Postcritique des Plaques Utilisees en Construction Metalique*. Memoires de la Societe Royale des Sciences de Liege, 5me serte, tome VIII, fasc. 5, pp. 64–68, 103, 104.
2. W. J. Supple, Changes of wave-form of plates in the postbuckling range. *Int. J. Solids Structures* **6**, 1243–1258 (1970).
3. W. J. Supple, On the change in the buckle pattern in elastic structures. *Int. J. Mech. Sci.* **10**, 737–745 (1968).
4. J. M. T. Thompson, Catastrophe theory in mechanics: progress or digression. *J. Struct. Mech.* **10**, 167–175 (1982).
5. R. Magnus and T. Poston, On the full unfolding of the von Karman equations at a double eigenvalue. In Report of the Battelle Advanced Studies Centre, Geneva, Aug. 1977.
6. T. Poston and I. Stewart, *Catastrophy Theory and Its Applications*. Pitman, London (1978).
7. E. Byskov and J. W. Hutchinson, Mode interaction in axially stiffened cylindrical shells. AIAA J. **15**, (1977).
8. T. R. Graves-Smith, The ultimate strength of locally buckled columns of arbitrary length. *Thin Walled Steel Construction* (Edited by K. C. Rockey and H. V. Hill). Crosby Lockwood, London (1967).
9. A. van der Neut, The interaction of local buckling and column failure of thinwalled compression members. *Proc. 12th Int. Cong. Appl. Mech.*, Stanford University, pp. 389–399 (1968) Springer, Berlin (1969).
10. V. Tvergaard, Imperfection-sensitivity of a wide integrally stiffened panel under compression. *Int. J. Solids Structures* **9**, 177–192 (1973).
11. W. T. Koiter and G. D. C. Kuiken, The interaction between local buckling and overall buckling on the behavior of built up columns. WTHD Rep. **23**, Delft (1971).
12. W. T. Koiter and M. Pignataro, An alternative approach to the interaction between local and overall buckling in stiffened panels. *IUTAM Symp.* Cambridge, 1974, "Buckling of Structures," (Edited by B. Budiansky), pp. 133–148. Springer-Verlag, Berlin (1976).
13. W. T. Koiter and M. Pignataro, A general theory of interaction between local and overall buckling of stiffened panels. Rep. No. 353, Laboratory of Engineering Mechanics, Delft University of Technology (1977).
14. A. van der Neut, Mode of interaction in stiffened panels. *IUTAM Symp.*, Cambridge, 1974, "Buckling of Structures", (Edited by B. Budiansky), pp. 117–132. Springer-Verlag, Berlin (1976).
15. J. M. T. Thompson and G. M. Lewis, On the optimum design of thin walled compression members. *J. Mech. Phys. Solids* **20**, 101–109 (1972).
16. G. W. Hunt, Imperfection-sensitivity of semi-symmetric branching. *Proc. R. Soc., London*, Ser. **A357**, 193–211 (1977).
17. S. Sridharan and T. R. Graves-Smith, Post-buckling analyses with finite strips. *J. Engng. Mech. Div., ASCE*, **EM5**, 16551 (1981).
18. J. P. Benthem, The reduction in stiffness of combinations of rectangular plates in compression after exceeding the buckling load. NLL-Tr, S. 539 (June 1959).
19. B. Budiansky and J. W. Hutchinson, Dynamic buckling of imperfection-sensitive structures. *Proc. 11th Int. Cong. Appl. Mech.* Munchen, 1964, pp. 656–651. Springer, Berlin (1966).
20. S. Sridharan, A semianalytical method for the post-local-torsional buckling analysis of prismatic plate structures. *Int. J. Num. Meth. Engng.* **18**, 1685–1697 (1982).